

Effect of Nozzle Installation on The Aerodynamic Performance of A Savonius Vertical Axis Wind Turbine, Using CFD method

Ali Abjadi^{1*}, Farzad Ghafoorian², Sahel Chegini³

¹Department of Mechanical Engineering, South Tehran Branch, Islamic Azad University, Tehran, Iran.

²Turbomachinery Research Laboratory, Department of Energy Conversion, School of Mechanical Engineering, Iran University of Science and Technology, Tehran, Iran.

³School of Railway Engineering, Iran University of Science and Technology, Tehran, Iran.

Abstract

In low-velocity areas, the Savonius turbine offers an attractive, economical, and ecologically beneficial method of generating electricity. However, due to the fact that scientists are still looking for a solution to the primary issue of the Savonius turbine's poor efficiency, this turbine has not yet been properly investigated. To increase the efficiency of the Savonius turbine the nozzle system can be utilized. In the present study, a 2-dimensional numerical simulation using the computational fluid dynamics (CFD) method was conducted for a Savonius vertical axis wind turbine (VAWT). This study aims to investigate the effect of different nozzle installation angles and nozzle wall lengths on the performance of the Savonius turbine and for this purpose, six different nozzle designs are investigated. In order to observe the performance of the mentioned turbine, the power coefficient (C_p) is calculated, and their values are compared in the different tip speed ratios (TSR). The results show that the highest efficiency of Savonius VAWTs is achieved with a nozzle installation angle of 55° . After that in optimum nozzle installation angle, the nozzle length of 1900 mm exhibits better performance compared to other nozzle lengths at a TSR of 0.5.

Keywords: *vertical axis wind turbine; Savonius wind turbine; nozzle wall length, nozzle installation angle, power coefficient; CFD simulation; tip speed ratio*

* Corresponding author. Department of Mechanical Engineering, South Tehran Branch, Islamic Azad University, Tehran, Iran. E-mail address: a_abjadi@azad.ac.ir (Ali Abjadi).

Nomenclature			
Symbols		Subscript	
V	Inlet flow velocity (m/s)	T	Turbulence
N	Number of rotation (rpm)	Abbreviations	
M	Torque (N.m)	VAWT	Vertical axis wind turbine
P	Output power (W)	HAWT	Horizontal axis wind turbine
D _o	Rotor diameter (m)	CFD	Computational fluid dynamic
D	Buckets diameter (m)	TSR	Tip speed ratio
C _p	Power coefficient		
C _m	Torque coefficient		
e	Overlap size (m)		
H	Rotor height (m)		
Greek			
ρ	Density (kg/m ³)		
ψ	Helical angle		
ω	Angular velocity (rad/s)		

1. Introduction

Rising concerns about air pollution from excessive consumption of fossil fuels storages have led scientists to start researching about extracting clean energy from renewable sources like solar, wind, geothermal and hydro power energy sources. Meanwhile, wind energy was recognized as one of the cleanest renewable energy sources [1]. Wind turbines are divided into two general categories based on their rotating axis, vertical axis wind turbines (VAWTs) and horizontal axis wind turbines (HAWTs). Recently, VAWTs have grabbed the attention of engineers due to their ease of installation and independence in the wind flow direction and they are used are widely developed[2]. VAWTs are divided into two main categories. Rotors that work with drag force, such as Savonius VAWTs, and rotors which

operate with lift force, like H-type Darrieus and Gorlov VAWTs[3]. Drag base VAWTs have less power production capacity than lift base types, however, their independence from the initial torque and the self-starting ability have made them preferable[4]. It is obvious that the efforts of the researchers have been on increasing the efficiency and improving the aerodynamic performance of the VAWTs, for example, by applying geometric changes such as the number of blades, the blade chord length and the blade airfoil profile type on a Gorlov turbine, they have increased its power coefficient[5]. In Savonius VAWTs, the buckets geometry and configuration has a significant impact on the aerodynamic performance of the turbine. In a CFD study, the performance of the turbine was optimized by examining the optimal amount of buckets overlap[6]. In another CFD study, the effect of shape factor, which is associated with changing the buckets' configuration, was investigated and it was found that the innovative buckets' design led to an effective air flow direction between the blades and, as a result, improved performance[7]. Also, the buckets' arc angle optimal value has created a favorable pressure in the convex side of the blade, causing an increase in torque value and ultimately improving performance[8]. In addition to the rotor configuration, the air flow direction and the wind speed have a significant effect on the turbine performance and efficiency[9]. The increase in the wind speed, which has a direct effect on the increase in the Reynolds number, has been investigated on the increase in the efficiency of the Gorlov turbine, and it has been determined that the efficiency has increased with the raise in the wind speed and turbulence intensity[10]. Also, the presence of the curtain in the upstream part of the turbine leads to more effective air flow and the output power increases significantly[11]. It should be considered that the curtain length and its walls' position angle have a significant effect on the direction of the air flow and rotor aerodynamic performance, therefore, the walls' angle and their length are optimized[12]. A creative design of the deflector, which is a simple wall and a wall consisting of an airfoil profile, has been used to improve the air flow[13]. More complex forms of deflectors by turning the air flow and producing vortices and creating favorable pressure in the concave and convex areas of the rotor are also useful[14].

Placing the nozzle at an appropriate angle and distance from the rotor at the entrance of the wind tunnel and upstream of the rotor like a curtain and deflector also increases productivity[15].

The purpose of this study is to optimize the efficiency of a Savonius VAWT by deploying nozzle system at velocity inlet section and turbine upstream. For this purpose, different nozzle installation angles and nozzle wall lengths are investigated by studying the flow field characteristics around turbine and measuring turbine performance. Computational Fluid Dynamics (CFD) technique is adopted utilizing $k-\omega$ SST model, also numerical work had been carried out by employing Ansys Fluent.

2. Problem description and solution strategy

In this 2D CFD simulation a two-bladed Savonius VAWT is considered as the prototype and a simple rectangular is considered for modeling wind tunnel or stator domain. In this simulation the rotor outer interface is coupled with the inner interface of rectangular domain by adopting this approach the rotation of rotor can be simulated thus, mesh motion method is nominated for this CFD modeling. It should be noted that turbine shaft is omitted to simplify the numerical study. The schematic of examined Savonius VAWT is shown in Figure1 and the dimensions and geometrical features of rotor and stator is presented in Table1.

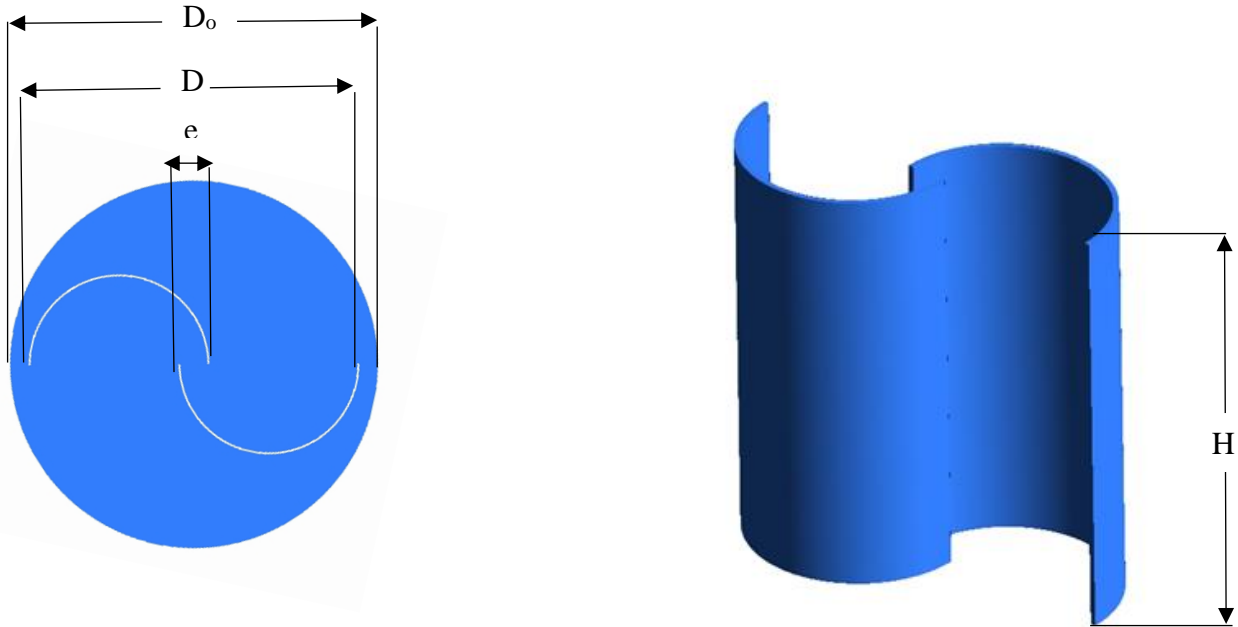


Figure 1 Schematic of Savonius VAWT

Table 1 Dimensions and main geometric characteristics of the simulated turbine rotor and stator.

	Quantity	Value
1	Number of blade	2
2	Bucket diameter	0.2(m)
3	Spacing size	0(m)
4	Overlap size	0.03(m)
5	Blade thickness	0.002(m)
6	Rotor diameter	0.37(m)
7	Height of blade	2D simulation
8	Length of stator	6(m)
9	Width of stator	2(m)

In current study an unstructured mesh method is adopted for both rotor and stator domains also for achieving more accurate and reliable results the grid size around the inner and outer interfaces was smaller than rotor and stator grids size also for avoiding flow separation around the buckets, not only

mesh size is get smaller but also boundary layer mesh is chosen by nominating inflation around the buckets, air flow velocity in this area is controlled. The mesh for this prototype is given in Figure 2.

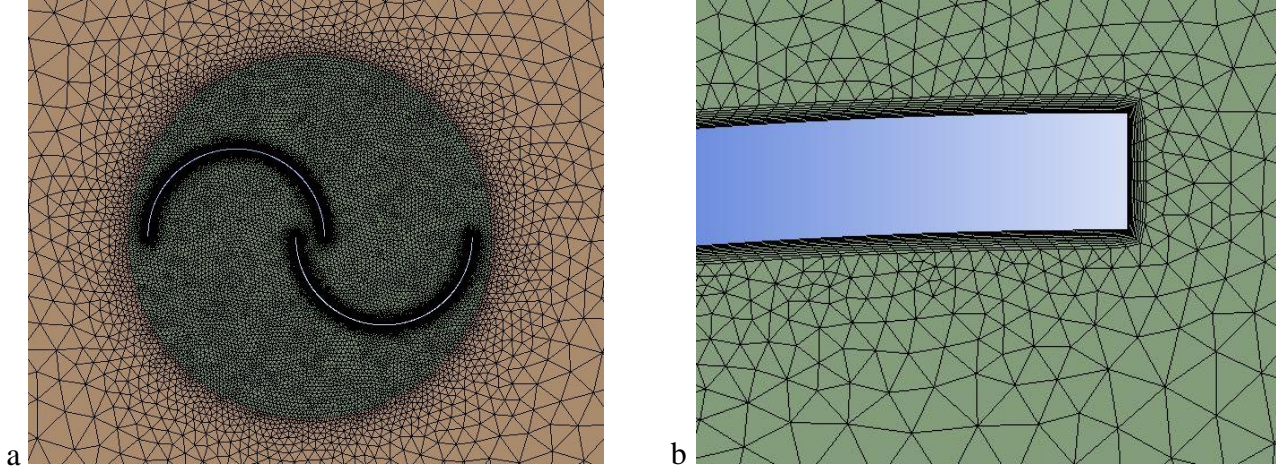


Figure 2 a) Rotor mesh, b) Blade boundary layer mes

3. Governing equations

In this 2D CFD analysis, the Navier-Stokes equation simulates the fluid flow around the Savonius VAWT rotor and buckets also, Reynolds averaging is used for current numerical modeling, and the velocity is divided into two terms, \bar{u} and u' , which are averaged and the fluctuating velocity terms. Also, equations 3 and 4 represent the Unsteady Reynolds Average Navier Stokes (URANS)[16].

$$\bar{u} = \frac{1}{T} \int_T u(t) dt \quad [16] \quad (1)$$

$$u' = u - \bar{u} \quad [16] \quad (2)$$

$$\frac{\partial \bar{u}_i}{\partial x_i} = 0 \quad [16] \quad (3)$$

$$\frac{\partial \bar{u}_i}{\partial t} + \bar{u}_j \frac{\partial \bar{u}_i}{\partial x_j} = -\frac{1}{\rho} \frac{\partial \bar{p}}{\partial x_i} + \nu \frac{\partial^2 \bar{u}_i}{\partial x_j^2} - \overline{u'_j \frac{\partial u'_i}{\partial x_j}} \quad [16] \quad (4)$$

Where u is the velocity of fluid flow (m/s) in x direction, p is pressure (Pa), and ρ (kg/m^3) is the fluid density.

Choosing Turbulence model is very crucial due to flow separation and great pressure gradient which have remarkable impact on CFD results. There are several common used turbulence models such as k - ϵ , k - ω , SST transition. These models use the Boussinesq assumption shown in Equation 5 for Reynolds stresses[17].

$$\tau_{ij} = 2\mu_t \left(S_{ij} - \frac{1}{3} \frac{\partial u_k}{\partial x_k} \delta_{ij} \right) - \frac{2}{3} \rho k \delta_{ij} \quad [17] \quad (5)$$

$$S_{ij} = \frac{1}{2} \left(\frac{\partial u_i}{\partial x_j} + \frac{\partial u_j}{\partial x_i} \right) \quad [17] \quad (6)$$

The k - ω SST model was used because this model can reduce the computational costs. Also, this approach is widely used for modeling the flow around turbomachines, also the k - ω SST equations for applications near walls regions are suitable[18]. These models are based on transport equations for the turbulence kinetic energy, k , and its dissipation rate ϵ . The model uses the following transport equations:

$$\frac{Dk}{Dt} = P - \beta^* \rho \omega k + \frac{\partial}{\partial x_j} \left[\left(\mu + \sigma_k \frac{\rho k}{\omega} \right) \frac{\partial k}{\partial x_j} \right] \quad [17] \quad (7)$$

$$\frac{D\omega}{Dt} = \frac{\gamma \omega}{k} P - \beta \rho \omega^2 + \frac{\partial}{\partial x_j} \left[\left(\mu + \sigma_\omega \frac{\rho k}{\omega} \right) \frac{\partial \omega}{\partial x_j} \right] \quad [17] \quad (8)$$

Where

$$P = \tau_{ij} \frac{\partial u_i}{\partial x_j} \quad [17] \quad (9)$$

τ_{ij} derived from equations 5 and 6.

The turbulent viscosity is assumed from the below equation:

$$\mu_t = \frac{\rho k}{\omega} [17] \quad (10)$$

The other parameters of the above equation are obtained from Table2.

Table 2 Constants of model k- ω [19]

C_μ	σ_k	σ_ω	β^*	β	γ
0.9	0.5	0.5	0.09	0.072	0.52

The γ coefficient was selected in order to obtain the appropriate value for the von Karmen constant ($\kappa \approx 0.41$), via the expression 11:

$$\gamma = \frac{\beta}{\beta^*} - \frac{\sigma_\omega k^2}{\sqrt{\beta^*}} [17] \quad (11)$$

The tip speed ratio is defined as the ratio between the blade tip speed and the wind speed (V_w). [16].

$$TSR = \frac{R \times \omega}{V_w} [16] \quad (12)$$

Where R is the radius and ω is the angular velocity of the rotor.

The torque coefficient (C_m) and power coefficient (C_p) which is relation between product of rotor torque and angular velocity with wind power can be written as follows:

$$C_m = \frac{T}{\frac{1}{2} \rho A R V_w^2} [20] \quad (13)$$

$$C_p = \frac{P}{\frac{1}{2} \rho A V_w^3} [20] \quad (14)$$

Where ρ (kg/m^3) wind densities, V_w (m/s) is wind speeds entering the turbine, T (N.m) is turbine torque, P (W) is the extractable power, and A (m^2) is the swept area.

4. Numerical modeling and simulation

4.1. Boundary condition

For this 2D CFD modeling Ansys Fluent software was selected application benefits from finite volume method for solving equation. The finite volume method (FVM) is a method for representing and evaluating partial differential equations in the form of algebraic equations. In the finite volume method, volume integrals in a partial differential equation that contain a divergence term are converted to surface integrals, using the divergence theorem[21]. Since the unsteady physics of this modeling and the interaction between the buckets' movement and wake flow around the rotor blades, the transient approach was adopted. The velocity inlet boundary condition was selected for the stator inlet section which is located in the upstream section of rotor, and the outlet zone of the stator domain in the turbine downstream is defined as the pressure outlet condition. In mentioned 2D-CFD simulation SIMPLE scheme was selected, and second-order upwind spatial discretization was obtained for pressure, momentum, and turbulence equations.

4.2. Validation and Grid independence

The experimental study of a small-scale Savonius VAWT with two buckets performed by Wenehenubun etal. [22], was nominated for this CFD investigation. Regarding the experimental outputs, the inlet velocity of the wind tunnel was 10(m/s)[22]; thus, this amount was considered for inlet boundary condition for current simulation. The numerical information is compared to experimental informations at four different TSR values in order to verify the present numerical simulation. The validation results for C_p are shown in Figure 3.

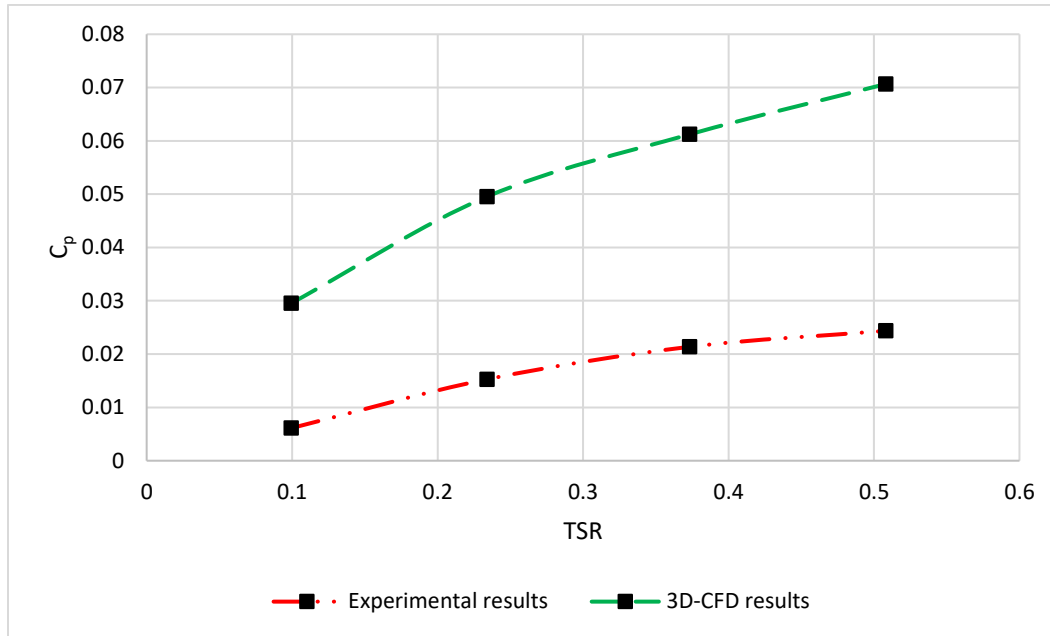


Figure 3 C_p values of CFD simulation compared to the experimental study results.

Regarding the information of Figure 3 CFD results have the same trend with the experimental data and they have an acceptable agreement. This fact indicates that the CFD investigation is reliable and numerical simulation is validated, however; the main root of the error between CFD and experimental data is related to omitting shaft and arms, therefore mechanical losses cannot be calculated in this CFD modeling also, 2D approach leads to an increase in the error between CFD and Experimental data, however; as this method is not time consuming, it can be adopted. Another essential action in order to clarify the accuracy of CFD simulation is grid independence. To achieve this goal the model mesh should be fine and C_p values in a certain point (TSR=0.23) must be evaluated for different grid numbers. In this study three different cases are considered. Element number for case1, case2 and case3 is about 250000, 350000 and 450000 respectively. The results of mesh independence are presented in Table 3.

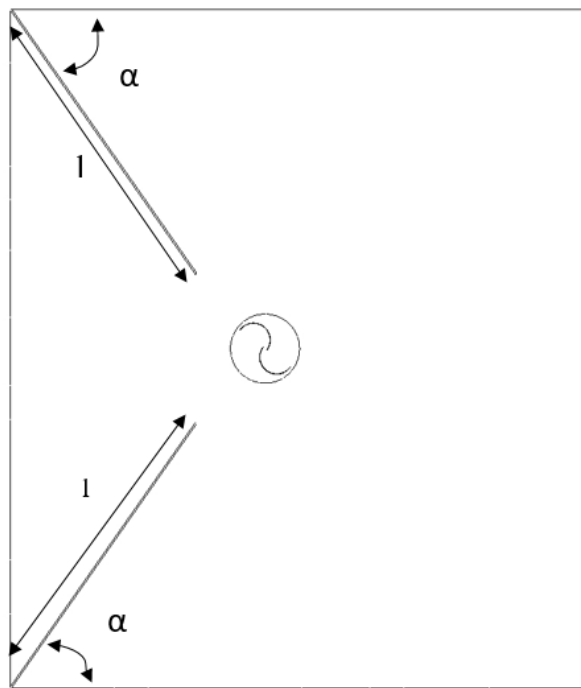
Table 3 Grid independence analysis results.

	Case	C_p value
1	Case 1	0.049
2	Case 2	0.046
3	Case 3	0.043

Based on Table 3 information, the C_p values are not sensibly different in the three cases, it means that the CFD simulation is not dependent on the number of grids and it again shows the accuracy of modeling.

5. Results and discussion

In this chapter, the nozzle is added to the inlet section of domain in the upstream of the rotor in order to guiding air flow to the rotor in a more effective way. The schematic of a Savonius VAWT with considering nozzle in shown in Figure 4.

**Figure 4** Savonius VAWT in presence of nozzle

Based on the Figure 4, nozzle which installed in the velocity inlet section has two walls which play significant role in directing air flow in an appropriate way to the rotor suction side thus the length size and the installation angle is really important. The nozzle installation angle, denoted by α , is the angle between the walls of the stator and the wall of the nozzle which will be examined further. In this chapter firstly, the effect of installation angle is numerically examined and when optimum angle is find as the second step the effect of nozzle arms will investigate.

5.1. Effect of Nozzle installation Angle

For examining the effect of nozzle installation angle three different angle values of 35° , 45° and 55° are considered in a constant length of 1500 (mm) and their effect on air flow direction and subsequently on the aerodynamic performance and the efficiency of the turbine is investigated. The results of the effect of different installation angle values on C_p is given in Figure 5.

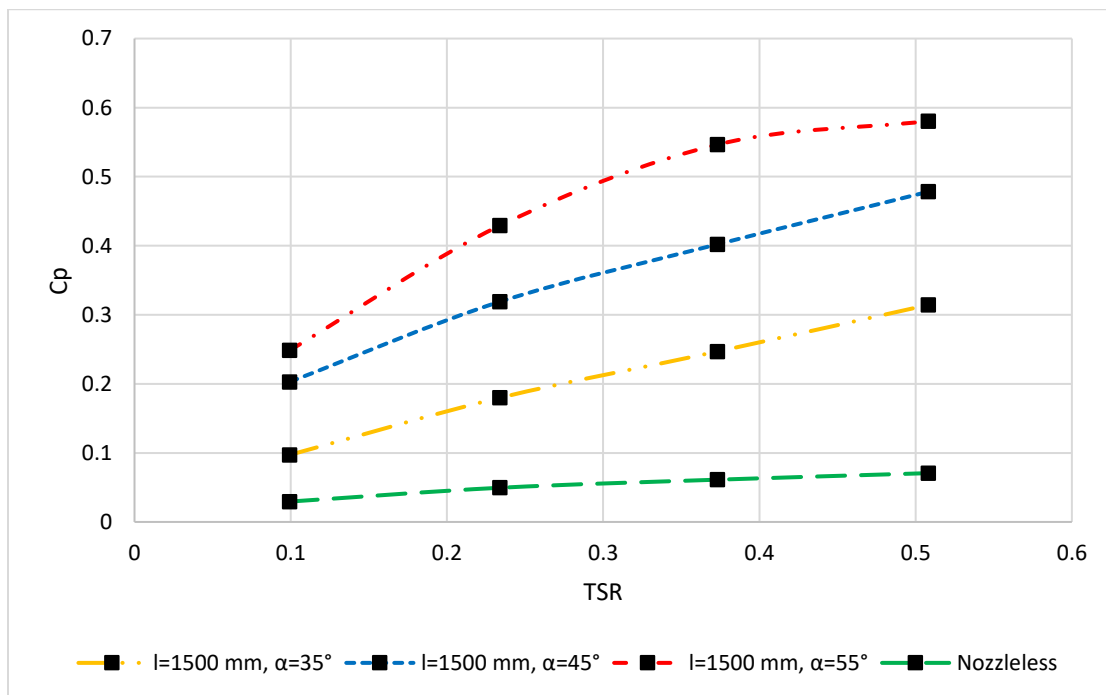


Figure 5 Effect of nozzle angle installation on C_p

Regarding the information of Figure 5 adding nozzle in the upstream section of rotor and in the velocity in let leads to a remarkable increase in C_p values and as a result by installing nozzle generated power is grew. Another reason for this increase in efficiency is the significant increase in the velocity value and subsequently increase in Reynolds number and turbulence intensity. Also it can be seen by raising α values the area of discharge section of nozzle decreased and it caused less air discharging form this section but in a more appropriate direction towards the rotor and the air flow focuses on the rotor upstream side and this situation causes free airflow stream to cover more parts of the rotor. Also, excessively narrowing the discharge section of the nozzle not only causes the air flow exit properly, but also preventing an unfavorable pressure gradient in the upstream zoon of the turbine rotor. For more clarity, the pressure and velocity contours are shown in Figure 6.

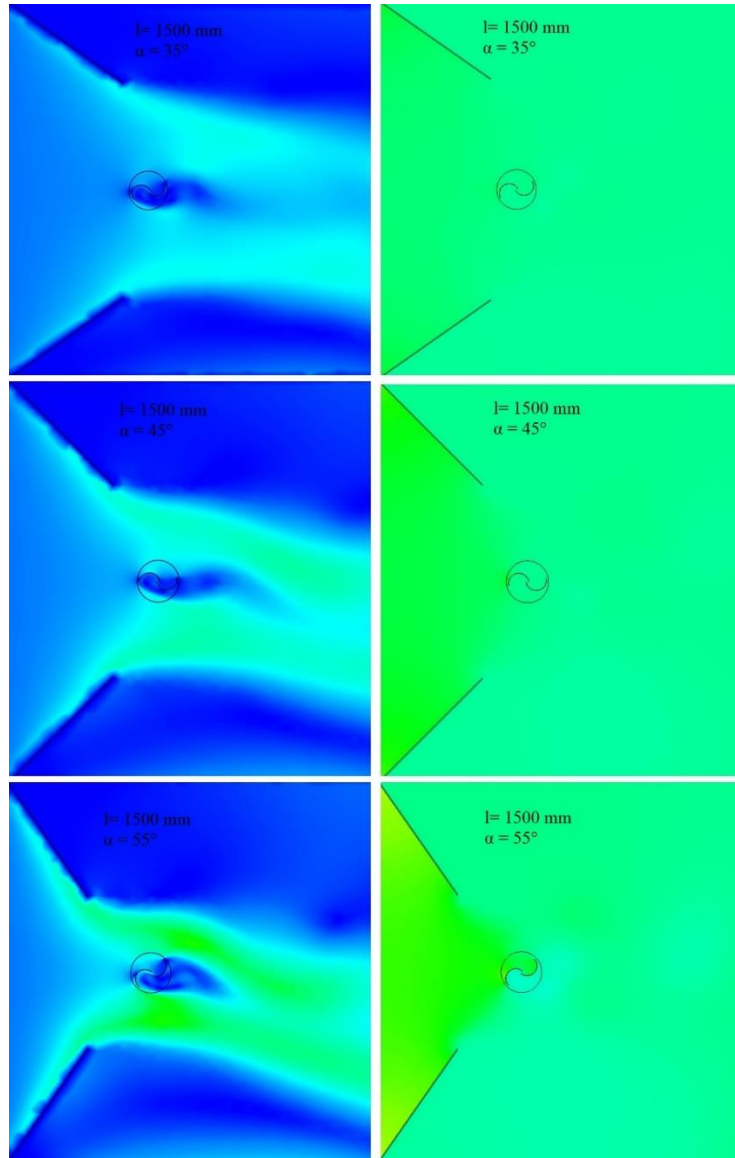


Figure 6 Velocity and pressure contour plots for different nozzle installation angle at TSR=0.5

Based on Figure 6 when nozzle installation angle is 55° air flow velocity is more than other conditions which leads to a remarkable raise in C_p values and generated power also wake flow region which is considered as low-speed zone is more instance in the downstream section and between buckets when the angle is smaller than 55° . This low speed zone and wake flow causes a reduction in turbine performance. Also Regarding pressure contour when angle is equal to 55° favorable pressure behind the nozzle discharge section and in the turbine rotor upstream side is more sensible than other angle of installation

values also in this configuration favorable pressure gradient in the concave and convex side of buckets which prepares drag force is more than other configurations.

As most effective angle of installation was equal to 55° , the effect of different wall length was investigated in this condition. To achieve this aim two different length values of 1300 (mm) and 1500 (mm) is studied beside the length of 1500 (mm). The results of the effect of different wall length on C_p is given in Figure 7.

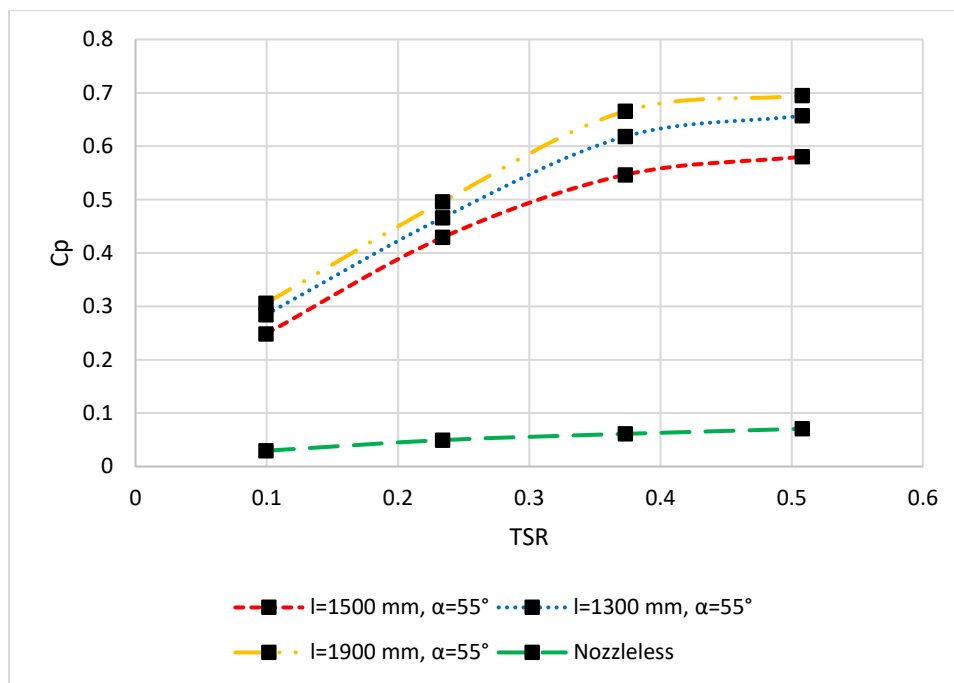


Figure 7 Effect of nozzle wall length on C_p

Based on the Figure 8 outputs by raising the nozzle walls length, C_p values increased significantly and also by looking at the details in higher rotational speeds or larger TSR values the increase in C_p values are more sensible. Also it should be noted when nozzle wall length grew and it installed closer to the upstream rotor section free air flow stream directed properly and also Reynolds number and turbulence intensity rose in this condition. For more clarity, the pressure and velocity contours are shown in Figure 8.

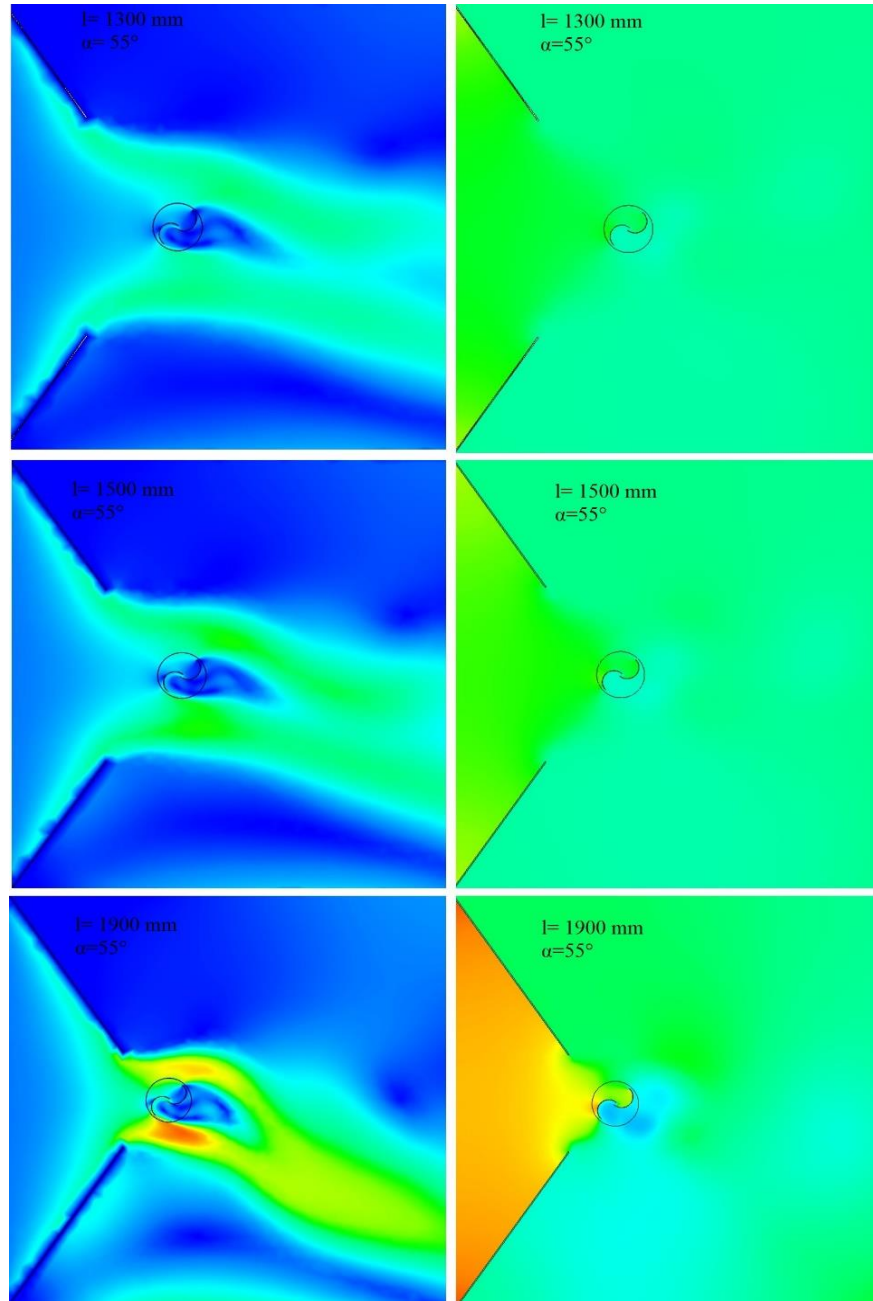


Figure 8 Velocity and pressure contour plots for different nozzle wall length at TSR=0.5

Looking at Figure 8 when nozzle wall length increased the discharge section of it came close to the turbine rotor section the wake flow and low-speed zone declined significantly in the downstream section of turbine and between buckets which boosted turbine performance and C_p values it means flow passed the turbine with higher speed. Also based on the pressure contour plots when wall length is equal to 1900

(mm) favorable pressure gradient is on the concave and convex section of buckets are more than other conditions which increase rotor overall torque and subsequently generated power. On the other hand when wall length increased, positive pressure behind the nozzle suction is grew which prove this fact that air flow directed to the rotor properly.

6. Conclusion

In this study, a numerical simulation based on CFD method was performed on the effect of installation a nozzle at velocity inlet section and turbine upstream. The effect of different nozzle installation angle was investigated in the first step and based on the C_p values in different rotational speed values and TSRs it was found the best angle value is relate to 55° and also favorable pressure and velocity which are important for aerodynamic performance and efficiency was increased in this condition. In the next step in the optimum nozzle installation angle value, the effect of nozzle wall length was examined and it was claimed that the most appropriate value is relate to 1900 (mm) which causes more favorable pressure and concave and convex side and subsequently more generated power.

References

- [1] S. L. Dixon and C. A. Hall, *Fluid mechanics and thermodynamics of turbomachinery*, Seventh edition. Amsterdam ; Boston: Butterworth-Heinemann is an imprint of Elsevier, 2014.
- [2] B. Hand, "A review on the historical development of the lift-type vertical axis wind turbine_ From onshore to offshore floating application," *Sustainable Energy Technologies and Assessments*, p. 11, 2020.
- [3] M. M. Aslam Bhutta, N. Hayat, A. U. Farooq, Z. Ali, Sh. R. Jamil, and Z. Hussain, "Vertical axis wind turbine – A review of various configurations and design techniques," *Renewable and Sustainable Energy Reviews*, vol. 16, no. 4, pp. 1926–1939, May 2012, doi: 10.1016/j.rser.2011.12.004.
- [4] M. Zemamou, M. Aggour, and A. Toumi, "Review of savonius wind turbine design and performance," *Energy Procedia*, vol. 141, pp. 383–388, Dec. 2017, doi: 10.1016/j.egypro.2017.11.047.
- [5] M. Akhlagi, F. Ghafoorian, M. Mehrpooya, and M. Sharifi Rizi, "Effective Parameters Optimization of a Small Scale Gorlov Wind Turbine, Using CFD Method," *Iranian Journal of Chemistry and Chemical Engineering*, 2022, doi: 10.30492/ijcce.2022.561960.5584.

- [6] M. Ebrahimpour, R. Shafaghat, R. Alamian, and M. S. Shadloo, "Numerical Investigation of the Savonius Vertical Axis Wind Turbine and Evaluation of the Effect of the Overlap Parameter in Both Horizontal and Vertical Directions on Its Performance," p. 16, 2019.
- [7] I. B. Alit, "Effect of Overlapping Ratio, Blade Shape Factor, and Blade Arc Angle to modified Rotor Savonius performances," vol. 13, no. 1, p. 6, 2018.
- [8] F. Ghafoorian, "Simulation and validation in order to improve the performance of Gorlov vertical axis wind turbine," Iran University of Science and Technology, 2021.
- [9] M. Al-Ghriyah, S. Mohd1, and D. Djamal Hissein, "Review of the Recent Power Augmentation Techniques for the Savonius Wind Turbines," *ARFMTS*.
- [10] M. Moghimi and H. Motawej, "Investigation of Effective Parameters on Gorlov Vertical Axis Wind Turbine," *Fluid Dyn*, vol. 55, no. 3, pp. 345–363, May 2020, doi: 10.1134/S0015462820030106.
- [11] B. D. Altan and M. Atilgan, "The use of a curtain design to increase the performance level of a Savonius wind rotors," *Renewable Energy*, vol. 35, no. 4, pp. 821–829, Apr. 2010, doi: 10.1016/j.renene.2009.08.025.
- [12] B. D. Altan, M. Atilgan, and A. Özdamar, "An experimental study on improvement of a Savonius rotor performance with curtaining," *Experimental Thermal and Fluid Science*, vol. 32, no. 8, pp. 1673–1678, Sep. 2008, doi: 10.1016/j.expthermflusci.2008.06.006.
- [13] M. Mosbahi, A. Ayadi, Y. Chouaibi, Z. Driss, and T. Tucciarelli, "Performance study of a Helical Savonius hydrokinetic turbine with a new deflector system design," *Energy Conversion and Management*, vol. 194, pp. 55–74, Aug. 2019, doi: 10.1016/j.enconman.2019.04.080.
- [14] W. A. El-Askary, M. H. Nasef, A. A. AbdEL-hamid, and H. E. Gad, "Harvesting wind energy for improving performance of Savonius rotor," *Journal of Wind Engineering and Industrial Aerodynamics*, vol. 139, pp. 8–15, Apr. 2015, doi: 10.1016/j.jweia.2015.01.003.
- [15] S. Roy, P. Mukherjee, and U. K. Saha, "Aerodynamic Performance Evaluation of a Novel Savonius-Style Wind Turbine Under an Oriented Jet," in *ASME 2014 Gas Turbine India Conference*, New Delhi, India, Dec. 2014, p. V001T08A001. doi: 10.1115/GTINDIA2014-8152.
- [16] M. S. Siddiqui, A. Rasheed, T. Kvamsdal, and M. Tabib, "Effect of Turbulence Intensity on the Performance of an Offshore Vertical Axis Wind Turbine," *Energy Procedia*, vol. 80, pp. 312–320, 2015, doi: 10.1016/j.egypro.2015.11.435.
- [17] N. Stergiannis, C. Lacor, J. V. Beeck, and R. Donnelly, "CFD modelling approaches against single wind turbine wake measurements using RANS," *J. Phys.: Conf. Ser.*, vol. 753, p. 032062, Sep. 2016, doi: 10.1088/1742-6596/753/3/032062.
- [18] N. Liamis and Y. Lebert, "Implementation of a low Reynolds k-epsilon turbulence model in a 3D Navier-Stokes solver for turbomachinery flows," in *31st Joint Propulsion Conference and Exhibit*, San Diego, CA, U.S.A., Jul. 1995. doi: 10.2514/6.1995-2335.
- [19] R. H. Nichols, "Turbulence Models and Their Application to Complex Flows," p. 214, Apr. 2010.
- [20] Z. Mao and W. Tian, "Effect of the blade arc angle on the performance of a Savonius wind turbine," *Advances in Mechanical Engineering*, vol. 7, no. 5, p. 168781401558424, May 2015, doi: 10.1177/1687814015584247.
- [21] A. Bejan and A. D. Kraus, *Heat transfer handbook*. New York: J. Wiley, 2003.
- [22] F. Wenehenubun, A. Saputra, and H. Sutanto, "An Experimental Study on the Performance of Savonius Wind Turbines Related With The Number Of Blades," *Energy Procedia*, vol. 68, pp. 297–304, Apr. 2015, doi: 10.1016/j.egypro.2015.03.259.